This article has been accepted for inclusion in a future issue of this journal. Content is final as presented, with the exception of pagination.

Trajectory Tracking of Underactuated Surface Vessels: A Linear Algebra Approach

Mario Emanuel Serrano, Gustavo J. E. Scaglia, Sebastián Alejandro Godoy, Vicente Mut, and Oscar Alberto Ortiz

***Abstract*— This brief presents the design of a controller that allows an underactuated vessel to track a reference trajectory in the $x-y$ plane. A trajectory tracking controller designed originally for robotic systems is applied for underactuated surface ships. Such a model is represented by numerical methods and, from this approach, the control actions for an optimal operation of the system are obtained. Its main advantage is that the condition for the tracking error tends to zero, and the calculation of control actions are obtained solving a system of linear equations. The proofs of convergence to zero of the tracking error are presented here and complete the previous work of the authors. Simulation results show the good performance of the proposed control system.**

***Index Terms*— Control system design, linear algebra, nonlinear model, tracking trajectory control.**

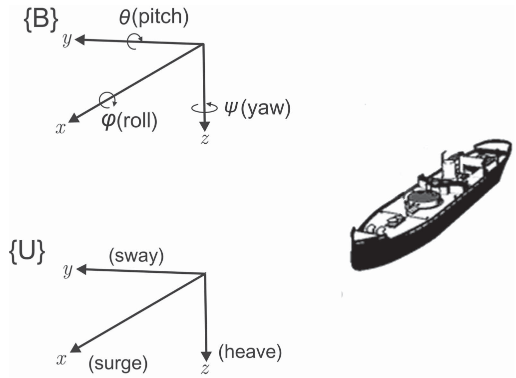

Fig. 1. Marine vessel: global coordinate frame {U} and a body-fixed coordinate frame {B}.

I. Introduction

THIS brief addresses the problem of trajectory tracking for an underactuated surface vessel (USV). The challenge of these problems appears relevant because of the fact that the motion of the USV in question possesses three degrees of freedom (yaw, sway, and surge neglecting the motion in roll, pitch and heave, see Fig. 1), whereas there are only two available controls (surge force and yaw moment). The use of trajectory tracking for a vessel system is justified in structured working spaces as well as in partially structured workspaces, where unexpected obstacles are found during the navigation. In the first case, the reference trajectory is set from a global trajectory planner. In the second case, the algorithms used to avoid obstacles usually replan the trajectory to avoid a collision, generating a new reference trajectory from this point on. In general, the goal is to find the combined control actions to track the reference trajectory, defined by the variables x_{ref} and y_{ref}.

The trajectory tracking control of the USV receives great attention from the control community in recent years. In the literature, different control strategies are proposed. Oh and Sun [1] proposed a model with predictive control scheme with line of sight for tacking problems of underactuated vessels based on linearization. In [2], a feedback controller that forced the ship to exponentially follow the desired trajectory from any initial conditions were shown.

Manuscript received August 22, 2012; revised June 5, 2013; accepted June 21, 2013. Manuscript received in final form June 24, 2013. This work was supported in part by the Consejo Nacional de Investigaciones Científicas y Técnicas, the National Council for Scientific Research, and the Universidad Nacional de San Juan, Argentina. Recommended by Associate Editor A. Alessandri.

The authors are with the National University of San Juan, San Juan 5400, Argentina (e-mail: serranoemanuel84@gmail.com; gscaglia@unsj.edu.ar; sgodoy@unsj.edu.ar; vmut@unsj.edu.ar; rortiz@unsj.edu.ar).

Digital Object Identifier 10.1109/TCST.2013.2271505

In [3], the authors proposed a single controller, called universal controller, which solved both the stabilization and tracking, simultaneously. An observer-controller scheme to track a trajectory in real time using the position and heading measurements of the ship were proposed in [4].

On the basis of Lyapunov's direct method and passivity scheme, Jiang [5] proposed two constructive tracking solutions for the underactuated ship. However, both Jiang [5] and Do *et al.* [6] imposed the yaw velocity to be nonzero. Ghommam *et al.* [7] considered the problem of controlling the plane position and orientation of an autonomous surface vessel using two independent side thrusters. Two transformations are introduced to represent the system into a pure cascade form. A discontinuous backstepping approach is then employed for the stabilization of the chained form system via a partial-state feedback. In [8], a controller was obtained based on Lyapunov's direct method and backstepping technique. A similar control strategy, which is also based on backstepping and Lyapunov synthesis, was proposed in [9]. The authors consider the problem of tracking a desired trajectory for fully actuated ocean vessels, in the presence of uncertainties and unknown disturbances. Similar ideas were also found in [10], an adaptive dynamical sliding mode controller based on backstepping method and dynamical sliding mode control theory was presented. Lapierre and Jouvencel [11] presented a robust nonlinear controller designed for driving an autonomous underwater vehicle onto a predefined path at constant forward speed. In most existing backstepping-based techniques, a very restrictive assumption is that yaw reference velocity must satisfy persistent excitation conditions and thus, it does not converge to zero. Consequently, a vessel cannot track straight-line reference trajectories, which renders unrealistic practice.

This brief provides a positive answer to the above challenging problem. A trajectory tracking controller, designed

This article has been accepted for inclusion in a future issue of this journal. Content is final as presented, with the exception of pagination.

originally for robotic systems [12]–[14], is applied for an underactuated surface ships. This simple approach suggests that knowing the value of the desired state, we can find a value for the control action, which forces the system to move itself from its current state to the desired one. The main contribution of this brief is that the proposed methodology is based on easily understandable concepts, and there is no need of complex calculations to attain the control signal. The algorithm can be implemented directly on the ship's microcontroller without the need to implement it on an external computer, because the calculations are simple to perform. This avoids the need to have an external computer and it also avoids problems that may arise in the communication between the external computer and the surface vessel. The methodology developed for tracking the reference trajectory (x_{ref} and y_{ref}) is based on determining the desired trajectories of the remaining state variables. These variable states are determined by analyzing the conditions for a system of linear equations to have an exact solution. Therefore, the control signals are obtained by solving the system of linear equations. The main advantage of this approach is the simplicity of the controller, and the use of discrete-time equations, which for its implementation on a computer system becomes natural. Also, to complete the previous work of the authors, the proof of the zero-convergence of the tracking error is included in this brief.

This brief is organized as follows. In Section II, the dynamic model of a underactuated surface ship is presented. The methodology of the controller design is shown in Section III. In Section IV, the theoretical results are validated with simulation results of the control algorithm. Finally, Section V presents the conclusion and some topics that are addressed in future contributions.

II. Dynamic Model of a Marine Vessel

A. Ship Model

Marine vessels require six independent coordinates to determine their complete configuration (position and orientation). The six different motion components are conveniently defined as surge, sway, heave, roll, pitch, and yaw (see Fig. 1). It is common to reduce the general six degrees of freedom model to motion in surge, sway, and yaw only. This is done by neglecting the heave, roll, and pitch modes, which are open loop stable for most ships. We consider marine surface vessels described by the three-DOF model (see [15])

$$\dot{x} = u\cos(\psi) - \upsilon\sin(\psi) \tag{1}$$
$$\dot{y} = u\sin(\psi) + \upsilon\cos(\psi)$$
$$\dot{\psi} = r \tag{2}$$
$$\boldsymbol{B}\boldsymbol{f} = \boldsymbol{M}\dot{\boldsymbol{\upsilon}} + \boldsymbol{C}(\boldsymbol{\upsilon})\boldsymbol{\upsilon} + \boldsymbol{D}\boldsymbol{\upsilon} \tag{3}$$

where $\boldsymbol{n} = [x, y, \psi]^T$ represents the earth-fixed position and heading, $\boldsymbol{\upsilon} = [u, \upsilon, r]^T \in R^3$ represents the vessel-fixed velocities, $\boldsymbol{M}$ is the vessel inertia matrix, $\boldsymbol{C}(\boldsymbol{\upsilon})$ is the centrifugal and coriolis matrix, $\boldsymbol{D}$ is the hydrodynamic damping matrix, the vector $\boldsymbol{f} = [T_u, T_r]^T$ is the control input vector, where T_u is the surge control and T_r is the yaw control, respectively. The mass and inertia matrix are assumed to be symmetric and positively definite. In particular, the matrixes $\boldsymbol{M}$ and $\boldsymbol{D}$ are assumed to have the following structure (see [16]):

$$\boldsymbol{M} \triangleq \begin{bmatrix} m_{11} & 0 & 0 \\ 0 & m_{22} & m_{23} \\ 0 & m_{23} & m_{33} \end{bmatrix} = \boldsymbol{M}^T > 0, \quad \boldsymbol{D} \triangleq \begin{bmatrix} d_{11} & 0 & 0 \\ 0 & d_{22} & d_{23} \\ 0 & d_{32} & d_{33} \end{bmatrix}. \tag{4}$$

The particular structure chosen for $\boldsymbol{M}$ and $\boldsymbol{D}$ is motivated by the fact that most marine surface vessels are port-starboard symmetric. In this case, the surge mode is decoupled from the sway-yaw subsystem, as it can be seen in (4). With the particular structure of the mass and inertia matrix $\boldsymbol{M}$ given in (4), the Coriolis and centripetal matrix $\boldsymbol{C}(\boldsymbol{\upsilon})$ is parameterized as in (5) (see [15]). The matrix $\boldsymbol{B}$ is the actuator matrix, it maps the control inputs and the real control forces and moments that act on the vessel

$$\boldsymbol{C}(\boldsymbol{\upsilon}) \triangleq \begin{bmatrix} 0 & 0 & -m_{22}\upsilon - m_{23}r \\ 0 & 0 & m_{11}u \\ m_{22}\upsilon + m_{23}r & -m_{11}u & 0 \end{bmatrix}$$
$$\boldsymbol{B} \triangleq \begin{bmatrix} b_{11} & 0 \\ 0 & 0 \\ 0 & b_{32} \end{bmatrix}. \tag{5}$$

The skew-symmetric property of the $\boldsymbol{C}(\boldsymbol{\upsilon})$ matrix simply implies the physical fact that centrifugal and Coriolis forces and moments do not contribute to the kinetic energy of the vessel.

Finally, we get

$$\begin{aligned} \dot{x} &= u\cos(\psi) - \upsilon\sin(\psi) \\ \dot{y} &= u\sin(\psi) + \upsilon\cos(\psi) \\ \dot{\psi} &= r \\ \dot{u} &= \frac{m_{22}}{m_{11}}\upsilon r + \frac{m_{23}}{m_{11}}r^2 - \frac{d_{11}}{m_{11}}u + \frac{b_{11}}{m_{11}}T_u \\ \dot{\upsilon} &= -\left(\frac{m_{23}}{m_{22}}\dot{r} - \frac{m_{11}}{m_{22}}ur - \frac{d_{22}}{m_{22}}\upsilon - \frac{d_{23}}{m_{22}}r\right) \\ \dot{r} &= -\frac{m_{23}}{m_{33}}\dot{\upsilon} + \frac{m_{11} - m_{22}}{m_{33}}\upsilon u - \frac{m_{23}}{m_{33}}ru - \frac{d_{32}}{m_{33}}\upsilon \\ &\quad - \frac{d_{33}}{m_{33}}r + \frac{b_{32}}{m_{33}}T_r. \end{aligned} \tag{6}$$

From (6), replacing the sway acceleration $\dot{\upsilon}$ in yaw acceleration $\dot{r}$ (row six), the ship model is expressed as

$$\begin{aligned} \dot{x} &= u\cos(\psi) - \upsilon\sin(\psi) \\ \dot{y} &= u\sin(\psi) + \upsilon\cos(\psi) \\ \dot{\psi} &= r \\ \dot{u} &= \frac{m_{22}}{m_{11}}\upsilon r + \frac{m_{23}}{m_{11}}r^2 - \frac{d_{11}}{m_{11}}u + \frac{b_{11}}{m_{11}}T_u \\ \dot{r} &= \frac{m_{23}}{m_{33}}\left(\frac{m_{23}}{m_{22}}\dot{r} + \frac{m_{11}}{m_{22}}ur + \frac{d_{22}}{m_{22}}\upsilon + \frac{d_{23}}{m_{22}}r\right) \\ &\quad + \frac{m_{11} - m_{22}}{m_{33}}\upsilon u - \frac{m_{23}}{m_{33}}ru - \frac{d_{32}}{m_{33}}\upsilon - \frac{d_{33}}{m_{33}}r + \frac{b_{32}}{m_{33}}T_r. \end{aligned} \tag{7}$$

This article has been accepted for inclusion in a future issue of this journal. Content is final as presented, with the exception of pagination.

Finally, the equations that define the marine vessel model is written as

$$\begin{aligned}\dot{x} &= u\cos(\psi) - \upsilon\sin(\psi)\\ \dot{y} &= u\sin(\psi) + \upsilon\cos(\psi)\\ \dot{\psi} &= r\\ \dot{u} &= \frac{m_{22}}{m_{11}}\upsilon r + \frac{m_{23}}{m_{11}}r^2 - \frac{d_{11}}{m_{11}}u + \frac{b_{11}}{m_{11}}T_u\\ \dot{r} &= \frac{m_{22}}{m_{22}m_{33} - m_{23}^2}\\ &\quad\times\left((m_{11} - m_{22})\,\upsilon u + \left(\frac{m_{11}m_{23}}{m_{22}} - m_{23}\right)ru\right.\\ &\quad\left. + \left(\frac{d_{22}m_{23}}{m_{22}} - d_{32}\right)\upsilon + \left(\frac{d_{23}m_{23}}{m_{22}} - d_{33}\right)r + b_{32}T_r\right).\end{aligned} \tag{7}$$

III. Controller Design

A. Problem Statement

Let us consider the first-order differential equation

$$\frac{dy}{dt} = \dot{y} = f(y, t, u) \qquad y(0) = y_0 \tag{8}$$

where y represents the output to the system to be controlled, u the control action, and t the time. The values of $y(t)$ at discrete time $t = nT_0$, where T_0 is the sampling period and $n \in \{0, 1, 2, 3, \ldots\}$ is denoted as $y_{(n)}$. Thus when computing $y_{(n+1)}$ by knowing $y_{(n)}$, (1) should be integrated over the time interval $nT_0 \le t \le (n+1)T_0$ as follows:

$$y_{(n+1)} = y_{(n)} + \int_{nT_0}^{(n+1)T_0} f(y, t, u)dt \tag{9}$$

where u remains constant during the interval $nT_0 \le t < (n+1)T_0$. Therefore, if we know beforehand the reference trajectory (referred to as $y_{\text{ref}}(t)$) to be followed by $y(t)$, then $y_{(n+1)}$ is substituted by $y_{\text{ref}(n+1)}$ into (3), and it is possible to calculate $u_{(n)}$ that represents the control action required to go from the current state to the desired one.

There are several numerical integration methods to calculate $y_{(n+1)}$. For instance, the Euler method approaches can be used

$$y_{(n+1)} \cong y_{(n)} + T_0 f(y_{(n)}, t_{(n)}, u_{(n)}). \tag{10}$$

The use of numerical methods in the simulation of the system is based mainly on the possibility to determine the state of the system at instant $n+1$ from the state, control action, and other variables at instant n. Therefore, $y_{(n+1)}$ is substituted by a function of reference trajectory and then the control action to make the output system evolve from the current value ($y_{(n)}$) to the desired one can be calculated. Therefore, the approximation is used to find the best way to go from one state to the next, according to the availability of the system model.

In this brief, we apply this approach in the dynamic model of a marine vessel and thus obtain the control actions that allow the ship to follow a trajectory previously established. In Section II-A, the design of the proposed controller will be analyzed.

B. Controller Design

In this section, a control law capable of generating the signals $[T_u, T_r]$ is designed, with the objective that the ship position $[x(t), y(t)]$ follows the reference trajectory $[x_{\text{ref}}(t), y_{\text{ref}}(t)]$.

Then, (7) can be expressed in (11), as shown at the bottom of the page. When using the Euler approximation, we have (12), shown at the bottom of the page, or, in compact form as

$$\boldsymbol{A\tau} = \boldsymbol{b}. \tag{13}$$

Equation (13) represents a system of linear equations which allows at each sampling instant to calculate the control actions

$$\begin{bmatrix} 0 & 0\\ 0 & 0\\ 0 & 0\\ b_{11} & 0\\ 0 & b_{32}\end{bmatrix}\begin{bmatrix} T_u\\ T_r\end{bmatrix} = \begin{bmatrix} \dot{x} - u\cos(\psi) - \upsilon\sin(\psi)\\ \dot{y} - u\sin(\psi) + \upsilon\cos(\psi)\\ \dot{\psi} - r\\ m_{11}\dot{u} - m_{22}\upsilon r - m_{23}r^2 + d_{11}u\\ \frac{m_{22}m_{33}-m_{23}^2}{m_{22}}\dot{r} - (m_{11} - m_{22})\,\upsilon u - \left(\frac{m_{11}m_{23}}{m_{22}} - m_{23}\right)ru - \left(\frac{d_{22}m_{23}}{m_{22}} - d_{32}\right)\upsilon - \left(\frac{d_{23}m_{23}}{m_{22}} - d_{33}\right)r\end{bmatrix} \tag{11}$$

$$\underbrace{\begin{bmatrix} 0 & 0\\ 0 & 0\\ 0 & 0\\ b_{11} & 0\\ 0 & b_{32}\end{bmatrix}}_{\boldsymbol{A}}\underbrace{\begin{bmatrix} T_{u(n)}\\ T_{r(n)}\end{bmatrix}}_{\boldsymbol{\tau}}$$

$$= \underbrace{\begin{bmatrix} \frac{x_{(n+1)}-x_{(n)}}{T_0} - u_{(n)}\cos(\psi_{(n)}) - \upsilon_{(n)}\sin(\psi_{(n)})\\ \frac{y_{(n+1)}-y_{(n)}}{T_0} - u_{(n)}\sin(\psi_{(n)}) + \upsilon_{(n)}\cos(\psi_{(n)})\\ \frac{\psi_{(n+1)}-\psi_{(n)}}{T_0} - r_{(n)}\\ m_{11}\frac{u_{(n+1)}-u_{(n)}}{T_0} - m_{22}\upsilon_{(n)}r_{(n)} - m_{23}r_{(n)}^2 + d_{11}u_{(n)}\\ \left(\frac{m_{22}m_{33}-m_{23}^2}{m_{22}}\right)\frac{r_{(n+1)}-r_{(n)}}{T_0} - (m_{11} - m_{22})\upsilon_{(n)}u_{(n)} - \left(\frac{m_{11}m_{23}}{m_{22}} - m_{23}\right)r_{(n)}u_{(n)} - \left(\frac{d_{22}m_{23}}{m_{22}} - d_{32}\right)\upsilon_{(n)} - \left(\frac{d_{23}m_{23}}{m_{22}} - d_{33}\right)r_{(n)}\end{bmatrix}}_{\boldsymbol{b}}. \tag{12}$$

This article has been accepted for inclusion in a future issue of this journal. Content is final as presented, with the exception of pagination.

so that the ship achieves the reference trajectory. If the reference trajectory is given, $[x_{\text{ref}(n+1)}, y_{\text{ref}(n+1)}]^T$, then it can be taken into account to calculate the required control action $[T_u, T_r]^T$ that allows the marine vessel to evolve from the present position to the reference trajectory one. Now, it is necessary to specify the conditions for this system to have an exact solution.

From (12), it is seen that in order for the system of equations to have an exact solution, the rows of $\boldsymbol{b}$ corresponding to the zero rows of $\boldsymbol{A}$ must be equal to zero. Then, the first condition for the system of (12) to have exact solution is that the system of two equations and one unknown variables in (14) have exact solution

$$\begin{bmatrix} \cos(\psi_{(n)}) \\ \sin(\psi_{(n)}) \end{bmatrix} u_{(n)} = \begin{bmatrix} \left(\frac{x_{(n+1)}-x_n}{T_0}\right) + v_{(n)}\sin(\psi_{(n)}) \\ \left(\frac{y_{(n+1)}-y_{(n)}}{T_0}\right) - v_{(n)}\cos(\psi_{(n)}) \end{bmatrix}. \quad (14)$$

Then, the following expression is defined:

$$x_{(n+1)} = x_{\text{ref}(n+1)} - k_x(\underbrace{x_{\text{ref}(n)} - x_{(n)}}_{e_{x(n)}}) \quad (15)$$

$$y_{(n+1)} = y_{\text{ref}(n+1)} - k_y(\underbrace{y_{\text{ref}(n)} - y_{(n)}}_{e_{y(n)}}). \quad (16)$$

It is important to remark that the value of the difference between the reference and the real trajectory is called tracking error. It is given by $e_{x(n)} = x_{\text{ref}(n)} - x_{(n)}$ and $e_{y(n)} = y_{\text{ref}(n)} - y_{(n)}$; the tracking error is represented by $\|e_{(n)}\| = \sqrt{(e_{x(n)}^2 + e_{y(n)}^2)}$. In (15) and (16), the controller parameters fulfil $0 < k_x, k_y < 1$ so that the tracking error tends to zero when $n \to \infty$ (see Appendix section).

Considering (15) and (16), (14) can be expressed as follows:

$$\underbrace{\begin{bmatrix} \cos(\psi_{(n)}) \\ \sin(\psi_{(n)}) \end{bmatrix}}_{\boldsymbol{P}} \underbrace{u_{(n)}}_{s} = \underbrace{\begin{bmatrix} \left(\frac{x_{\text{ref}(n+1)}-k_x(x_{\text{ref}(n)}-x_{(n)})-x_{(n)}}{T_0}\right) + v_{(n)}\sin(\psi_{(n)}) \\ \left(\frac{y_{\text{ref}(n+1)}-k_y(y_{\text{ref}(n)}-y_{(n)})-y_{(n)}}{T_0}\right) - v_{(n)}\cos(\psi_{(n)}) \end{bmatrix}}_{\boldsymbol{q}}. \quad (17)$$

For the system, (17) has exact solution, the ship orientation must be

$$\tan(\psi_{ez}) = \frac{\sin(\psi_{ez(n)})}{\cos(\psi_{ez(n)})} = \frac{\frac{y_{\text{ref}(n+1)}-k_y(y_{\text{ref}(n)}-y_{(n)})-y_{(n)}}{T_0} - v_{(n)}\cos(\psi_{(n)})}{\frac{x_{\text{ref}(n+1)}-k_x(x_{\text{ref}(n)}-x_{(n)})-x_{(n)}}{T_0} + v_{(n)}\sin(\psi_{(n)})}. \quad (18)$$

The value of $\psi_{(n)}$ that satisfies (18) will be denominated $\psi_{ez(n)}$. It represents the ship orientation so that (18) has an exact solution. This orientation value allows the vessel reaches and follows the reference trajectory. Then, replacing $\psi_{(n)}$ by $\psi_{ez(n)}$ in the matrix $\boldsymbol{P}$ of (17)

$$\begin{bmatrix} \cos(\psi_{ez(n)}) \\ \sin(\psi_{ez(n)}) \end{bmatrix} u_{(n)} = \begin{bmatrix} \left(\frac{x_{\text{ref}(n+1)}-k_x(x_{\text{ref}(n)}-x_{(n)})-x_{(n)}}{T_0}\right) + v_{(n)}\sin(\psi_{(n)}) \\ \left(\frac{y_{\text{ref}(n+1)}-k_y(y_{\text{ref}(n)}-y_{(n)})-y_{(n)}}{T_0}\right) - v_{(n)}\cos(\psi_{(n)}) \end{bmatrix}. \quad (19)$$

The system (19) is of type $\boldsymbol{P}s = \boldsymbol{q}$ with more equations than unknowns, and its solution represent the surge velocity so that the tracking errors tends to zero. Its solution by least squares is obtained by solving the normal equations [17], $\boldsymbol{P}^T\boldsymbol{P}s = \boldsymbol{P}^T\boldsymbol{q}$, then the solution of (19) is expressed as

$$\begin{aligned} u_{ez} &= \left(\frac{y_{\text{ref}(n+1)} - k_y(y_{\text{ref}(n)} - y_{(n)}) - y_{(n)}}{T_0} - v_{(n)}\cos(\psi_{(n)})\right) \\ &\quad \times \sin(\psi_{ez(n)}) \\ &\quad + \left(\frac{x_{\text{ref}(n+1)} - k_x(x_{\text{ref}(n)} - x_{(n)}) - x_{(n)}}{T_0} + v_{(n)}\sin(\psi_{(n)})\right) \\ &\quad \times \cos(\psi_{ez(n)}). \end{aligned} \quad (20)$$

Now, the yaw velocity is analyzed. Considering the third row of (12) and (18), we define

$$r_{ez} = \frac{\psi_{ez(n+1)} - k_\psi \overbrace{(\psi_{ez(n)} - \psi_{(n)})}^{e_{\psi(n)}} - \psi_{(n)}}{T_0} \quad (21)$$

where $0 < k_\psi < 1$ to the tracking error tends to zero (see Appendix section). Then u_{ez} and r_{ez} represent the desired value of u and r so that the tracking errors ($e_{x(n)}$ and $e_{y(n)}$) tend to zero (see Appendix section).

Considering (20) and (21), to make the tracking error tends to zero, the following expression is defined:

$$\begin{aligned} u_{(n+1)} &= u_{ez(n+1)} - k_u\left(u_{ez(n)} - u_{(n)}\right) \\ r_{(n+1)} &= r_{ez(n+1)} - k_r\left(r_{ez(n)} - r_{(n)}\right) \end{aligned} \quad (22)$$

where $0 < k_u, k_r < 1$ so that the tracking error tends to zero (see Appendix section). Finally, by replacing (20)–(22) in the system (12), we find the next simplified system that allows to find the control actions that make that the tracking errors tend to zero as in (23), as shown at the bottom of the next page. Solving the system (23), it is possible to find the expression of the control actions in (24), as shown at the bottom of the next page.

Theorem 1: If the system behavior is ruled by (12) and the controller is designed by (18), (20), (21), and (24). Then $e_{(n)} \to 0, n \to \infty$ when trajectory tracking problems are considered.

The values of $T_{u(n)}$ and $T_{r(n)}$ represent the control actions necessary to meet the control goal. The proof of Theorem 1 and the convergence to zero of tracking errors are seen in Appendix. In the proposed methodology, the reference speeds are identified first so that the error tends to zero and then control actions are calculated to keep the velocity profile obtained. This controller structure arises naturally when the conditions for the system of (12) are analyzed to have an exact solution.

IV. SIMULATION RESULTS

This section presents three simulations of the ship, using the designed controller shown in Section III. The goal of the simulations is to confirm the good performance of the control law. The simulations are performed using a simulator developed in the MATLAB platform, which considers an accurate model

This article has been accepted for inclusion in a future issue of this journal. Content is final as presented, with the exception of pagination.

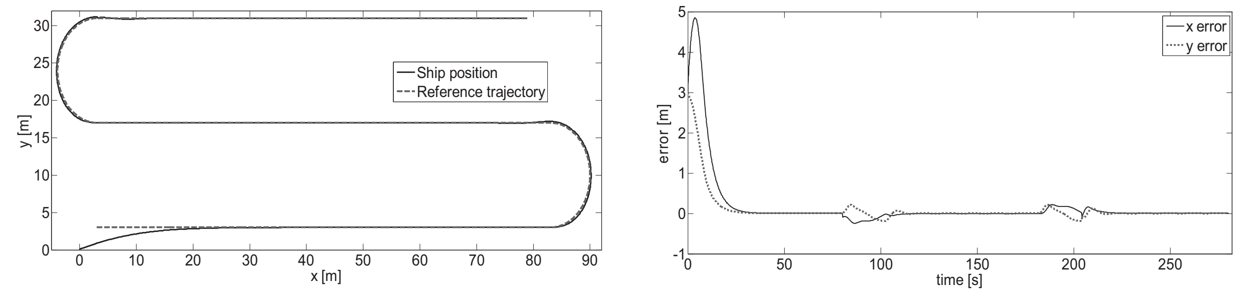

Fig. 2. Simulation results. (a) Tracking trajectory in the $x-y$ plane. (b) Tracking error.

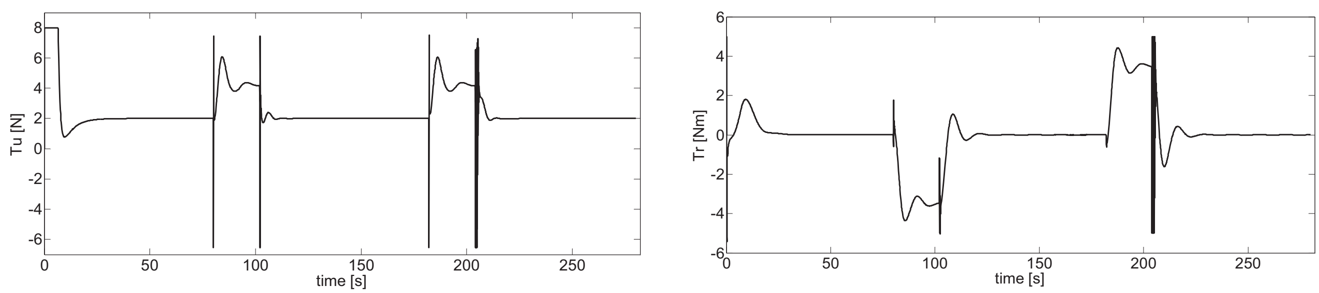

Fig. 3. Simulation results. (a) Control action T_u. (b) Control action T_r.

of the marine vessel. The control approach is applied on the original time-continuous system. The values of the parameters of the marine vessel were obtained from [15], where the model was identified about the center of gravity (CG), and translating this model to the desired body frame origins. The body origin is chosen at 25 cm aft of the bow, or 33.5 cm fore of the CG along the center line of the vessel

$$\boldsymbol{M} = \begin{pmatrix} 25.8 & 0 & 0 \\ 0 & 33.8 & -11.748 \\ 0 & -11.748 & 6.813 \end{pmatrix}$$

$$\boldsymbol{D} = \begin{pmatrix} 2 & 0 & 0 \\ 0 & 7 & -2.5425 \\ 0 & -2.5425 & 1.422 \end{pmatrix} \tag{25}$$

$$\boldsymbol{B} = \begin{pmatrix} 1 & 0 \\ 0 & 0 \\ 0 & 1 \end{pmatrix}. \tag{26}$$

The values of the constants of the controller are $\left[k_x \; k_y \; k_u \; k_r \; k_\psi \right] = \left[0.98 \; 0.98 \; 0.894 \; 0.894 \; 0.3 \right]$.

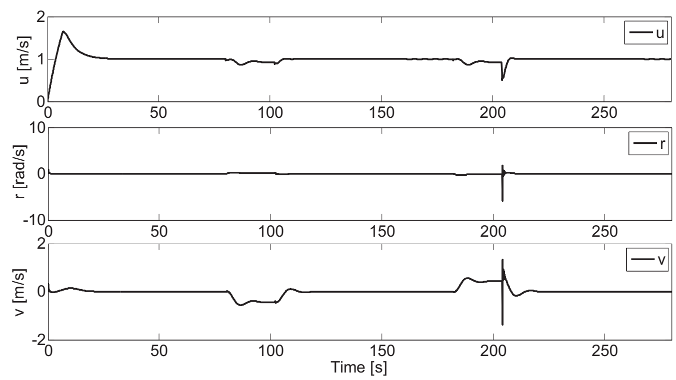

Fig. 4. Simulation results: surge, sway, and yaw velocities.

A. Trajectory Without Environmental Disturbances

To check the performance of the proposed controller, a trajectory consisting of a straight line generated with constant linear velocity and then followed by a semicircumference of 7 m radius is chosen. The trajectory is generated with a forward velocity of $u = 1$ m/s and a yaw velocity of $r = 0$ rad/s, and $r = 0.136$ rad/s, respectively. The reference

$$\begin{bmatrix} b_{11} & 0 \\ 0 & b_{32} \end{bmatrix} \begin{bmatrix} T_{u(n)} \\ T_{r(n)} \end{bmatrix} = \begin{bmatrix} m_{11} \frac{u_{ez(n+1)} - k_u \left(u_{ez(n)} - u_{(n)} \right) - u_{(n)}}{To} - m_{22} v_{(n)} r_{(n)} - m_{23} r_{(n)}^2 + d_{11} u_{(n)} \\ \left\{ \begin{array}{c} \left(m_{33} + \frac{m_{23}^2}{m_{22}} \right) \frac{r_{ez(n+1)} - k_r \left(r_{ez(n)} - r_{(n)} \right) - r_{(n)}}{To} - \left(m_{11} - m_{22} \right) v_{(n)} u_{(n)} \\ + \left(m_{23} - \frac{m_{11} m_{23}}{m_{22}} \right) r_{(n)} u_{(n)} + \left(d_{32} - \frac{d_{22} m_{23}}{m_{22}} \right) v_{(n)} + \left(d_{33} - \frac{d_{23} m_{23}}{m_{22}} \right) r_{(n)} \end{array} \right\} \end{bmatrix} \tag{23}$$

$$\begin{bmatrix} T_{u(n)} \\ T_{r(n)} \end{bmatrix} = \begin{bmatrix} \frac{1}{b_{11}} \left(m_{11} \frac{u_{ez(n+1)} - k_u \left(u_{ez(n)} - u_{(n)} \right) - u_{(n)}}{To} - m_{22} v_{(n)} r_{(n)} - m_{23} r_{(n)}^2 + d_{11} u_{(n)} \right) \\ \left\{ \begin{array}{c} \frac{1}{b_{32}} \left(\left(m_{33} + \frac{m_{23}^2}{m_{22}} \right) \frac{r_{ez(n+1)} - k_r \left(r_{ez(n)} - r_{(n)} \right) - r_{(n)}}{To} - \left(m_{11} - m_{22} \right) v_{(n)} u_{(n)} \right. \\ \left. + \left(m_{23} + \frac{m_{11} m_{23}}{m_{22}} \right) r_{(n)} u_{(n)} + \left(\frac{d_{22} m_{23}}{m_{22}} - d_{32} \right) v_{(n)} + \left(d_{33} + \frac{d_{23} m_{23}}{m_{22}} \right) r_{(n)} \right) \end{array} \right\} \end{bmatrix}. \tag{24}$$

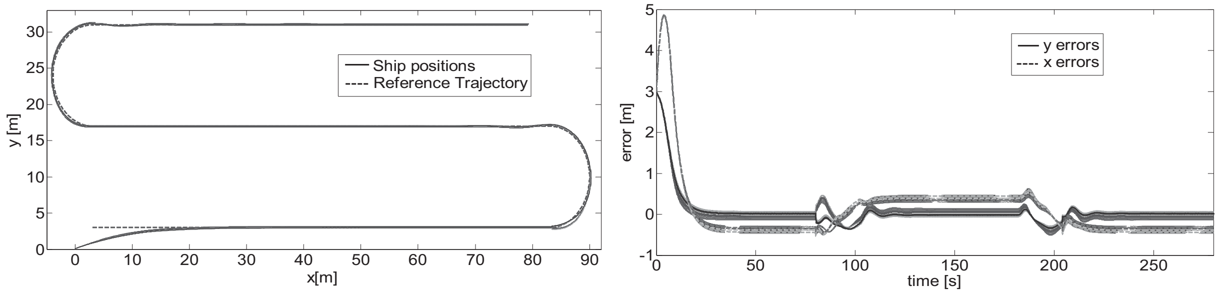

Fig. 5. Ship evolution whit environmental disturbance. (a) Tracking trajectory in the $x - y$ plane. (b) Tracking error.

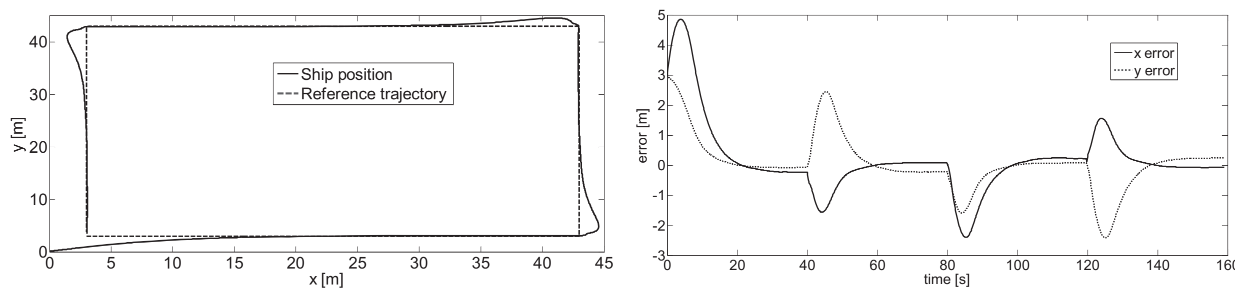

Fig. 6. Results of the simulation of square trajectory. (a) Tracking trajectory in the $x - y$ plane. (b) Tracking error.

trajectory starts at $(x_{\mathrm{ref}(0)}, y_{\mathrm{ref}(0)}) = (3\ \mathrm{m}, 3\ \mathrm{m})$, the sampling time T_0 used for the simulation is 0.1 s and the initial position of the ship is at the system origin. Fig. 2 shows that the ship tends to the reference trajectory and the error tends to zero. Fig. 2(a) shows how the ship reaches the reference trajectory quickly and then continues without undesirable oscillations. Fig. 2(b) shows how the tracking error tends to zero when there is a change in reference trajectory, which produces a slight increase of the tracking error, but later tends to zero. Fig. 3 shows how the control actions have no undesirable oscillations and how the control actions change to ensure that the tracking error tends to zero as can be seen in Fig. 2. Fig. 4 shows the ship velocity in surge, sway, and angular velocity in yaw. Note that the velocities remain bounded throughout the trajectory.

B. Trajectory With Environmental Disturbances

In the second simulation, the goal is to demonstrate the performance of the controller against environmental disturbances induced by wave, wind, and ocean current given by

$$\begin{aligned}
\dot{x} &= u\cos(\psi) - \upsilon\sin(\psi)\\
\dot{y} &= u\sin(\psi) + \upsilon\cos(\psi)\\
\dot{\psi} &= r\\
\dot{u} &= \frac{m_{22}}{m_{11}}\upsilon r + \frac{m_{23}}{m_{11}}r^2 - \frac{d_{11}}{m_{11}}u + \frac{b_{11}}{m_{11}}(T_u + T_{wu})\\
\dot{r} &= \frac{m_{22}}{m_{22}m_{33} - m_{23}^2}\\
&\quad\times\Bigg((m_{11} - m_{22})\upsilon u + \left(\frac{m_{11}m_{23}}{m_{22}} - m_{23}\right)ru\\
&\qquad + \left(\frac{d_{22}m_{23}}{m_{22}} - d_{32}\right)\upsilon + \left(\frac{d_{23}m_{23}}{m_{22}} - d_{33}\right)r\\
&\qquad + b_{32}(T_r + T_{wr})\Bigg).
\end{aligned}\tag{27}$$

Several simulations are performed to assess the effect of random disturbances of different level of intensity. Thus, Fig. 5 shows the result of 50 simulations, they are performed varying the disturbance level. These disturbances are given by $T_{wu} = 10^{-1}m_{11} + \lambda(\sin(10t) - 1)$ and $T_{wr} = 10^{-1}m_{33} + \lambda(\sin(10t) - 1)$, λ changes for each simulation according to $\lambda = \mathrm{rand}(\cdot)$, where $\mathrm{rand}(\cdot)$ is the random noise with a magnitude of one and zero lower bound. In Fig. 5(a), it is seen that the ship tends, in all cases, to the reference trajectory and after reaching the reference value, it keeps on without unwanted oscillations. Fig. 5(b) shows how all the tracking errors in x and y are small despite the perturbations. It is possible to see that there is a steady-state error. Nevertheless, the performance in the variables (x, y) is quite acceptable.

Finally, the simulation results with a square reference trajectory are shown in Figs. 6 and 7. Thus, the performance of the system, when the speed of the reference trajectory changes abruptly, is duly analyzed. The square reference trajectory is generated with a constant linear velocity of $u = 1$ m/s and a yaw velocity of $r = 0$ rad/s. The initial position of the ship is at the system origin and the trajectory begins in the position $(x_{\mathrm{ref}(0)}, y_{\mathrm{ref}(0)}) = (3\ \mathrm{m}, 3\ \mathrm{m})$. We assume that the environmental disturbances are generated similar to that of [2], $T_{wu} = 10^{-1}m_{11}\mathrm{rand}(\cdot)$ and $T_{wr} = 10^{-1}m_{11}\mathrm{rand}(\cdot)$, where $\mathrm{rand}(\cdot)$ is the random noise with a magnitude of one and zero lower bound. This choice results in nonzero mean disturbances. Fig. 6 represents the performance of the control law. Fig. 6(a) shows how the ship tends to the reference trajectory. Fig. 6(b) shows how the error tends to zero. When the desired trajectory suddenly changes its direction, it is sensible to expect a momentary increase of the error and then a later decrease. Values taken by the control actions so that the marine vessel follows the reference trajectory are shown in Fig. 7.

This article has been accepted for inclusion in a future issue of this journal. Content is final as presented, with the exception of pagination.

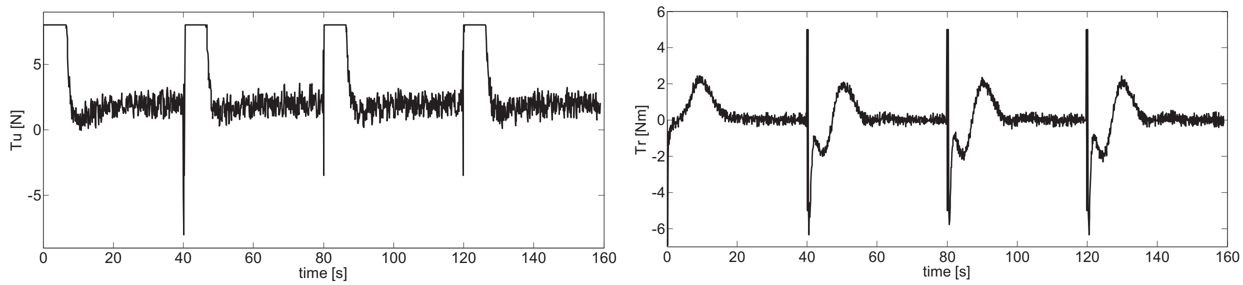

Fig. 7. Results of the simulation of square trajectory. (a) Control action T_u. (b) Control action T_r.

Fig. 6(b) shows that when the trajectory direction suddenly changes, the error increases, but it decreases afterwards. This trajectory-type is used to test the performance of the system, because it is a situation of worst case, where the error is acceptable.

V. Conclusion

In this brief, the trajectory tracking problem of the underactuated marine surface vessels were considered. Thus the design of a trajectory controller for a ship was presented. The design methodology is based on the search for conditions under which the system of linear equations had exact solution. These conditions established the desired values of orientation, linear speed, angular speed, and finally, the control actions so that the tracking error goes to zero, as shown in Appendix.

The proposed controller presented the advantages of being easy to design and to implement, the algorithm was implemented directly on the ship's microcontroller without the need of implementing it on an external computer, because the calculations are simple to perform. In comparison with previous published control laws [10]–[18], the method proposed here did not need a coordinate transformation. In addition, our controller did not present the disadvantage of [5] and [6] where it was imposed that the yaw velocity to be nonzero. Compared with [12]–[14], in this brief, the demonstration of convergence to zero of the tracking errors were included.

Simulation results showed the effectiveness of the proposed controller. The proposed controller was simple and presented an adequate level of robustness to disturbances, as shown in the simulation results. In addition, the developed methodology for the controller design was applied to other types of systems. The possibility to include the saturation of the control signals and observer-controller schemes, as shown in [3], in the formulation of the problem will be addressed in the future contributions.

Appendix

Proof of Theorem 1

If the system behavior is ruled by (12) and the controller is designed by (18), (20), (21), and (24). Then $e_{(n)} \to 0, n \to \infty$ when the trajectory tracking problems are considered. First, the analysis of other variables u, r and ψ are developed as follows.

The proof of convergence to zero of the tracking errors is started with a variable u. By replacing the control action $T_{u(n)}$, given by (24) in (12), the following expression is found:

$$\underbrace{u_{ez(n+1)} - u_{(n+1)}}_{e_{u(n+1)}} = k_u \underbrace{\left(u_{ez(n)} - u_{(n)}\right)}_{e_{u(n)}}. \tag{A.1}$$

Then

$$e_{u(n+1)} = k_u e_{u(n)} \tag{A.2}$$

where $0 < k_u < 1$, then $e_{u(n)} \to 0$, $n \to \infty$.

Using a similar procedure as above, the analysis of variable $e_{r(n)}$ is developed below. Then, considering (21) and (23) and replacing in (12)

$$\underbrace{r_{ez(n+1)} - r_{(n+1)}}_{e_{r(n+1)}} = k_r \underbrace{\left(r_{ez(n)} - r_{(n)}\right)}_{e_{r(n)}}. \tag{A.3}$$

Then

$$e_{r(n+1)} = k_r e_{r(n)} \tag{A.4}$$

where $0 < k_r < 1$, then $e_{r(n)}$, $n \to \infty$.

The same analysis applies to variable ψ. From (12) and (A.3)

$$\psi_{(n+1)} = \psi_{(n)} + T_0 \underbrace{\left(r_{ez(n)} - e_{r(n)}\right)}_{r_{(n)}}. \tag{A.5}$$

From (21) and (A.5)

$$\psi_{(n+1)} = \psi_{(n)} + T_0 \left(\frac{\psi_{ez(n+1)} - k_\psi \left(\psi_{ez(n)} - \psi_{(n)}\right) - \psi_{(n)}}{T_0} - e_{r(n)} \right). \tag{A.6}$$

Operating

$$\psi_{ez(n+1)} - \psi_{(n+1)} = k_\psi \left(\psi_{ez(n)} - \psi_{(n)}\right) \psi_{(n)} - T_0 e_{r(n)}. \tag{A.7}$$

Then

$$e_{\psi(n+1)} = k_\psi e_{\psi(n)} + T_0 e_{r(n)}. \tag{A.8}$$

Finally, how $0 < k_\psi < 1$ and $e_{r(n)} \to 0$ when $n \to \infty$, the guidance error $e\psi_n$ tend to 0 when $n \to \infty$.

Now, the convergence analysis of e_x and e_y is developed below.

From the corresponding equation of (12)

$$x_{(n+1)} = x_{(n)} + T_0 \left(u_{(n)} \cos(\psi_{(n)}) - v_{(n)} \sin(\psi_{(n)})\right). \tag{A.9}$$

Considering $e_{u(n)}$ from (A.1) and replacing in (A.9)

$$x_{(n+1)} = x_{(n)} + T_0 \left(u_{ez(n)} \cos(\psi_{(n)}) - v_{(n)} \sin(\psi_{(n)})\right) - T_0 e_{u(n)} \cos(\psi_{(n)}). \tag{A.10}$$

The Taylor approximation of $\cos(\psi_{(n)})$ in the desired value $\psi_{ez(n)}$ is

$$\cos(\psi_{(n)}) = \cos(\psi_{ez(n)}) - \sin\left(\psi_{ez(n)} + \zeta\left(\psi_{(n)} - \psi_{ez(n)}\right)\right)\left(\psi_{(n)} - \psi_{ez(n)}\right) \quad 0 < \zeta < 1. \tag{A.11}$$

Defining $e_{\psi(n)} = \psi_{ez(n)} - \psi_{(n)}$ as the error in ψ

$$\cos(\psi_{(n)}) = \cos(\psi_{ez(n)}) + \sin\left(\psi_{ez(n)} - \zeta e_{\psi(n)}\right) e_{\psi(n)} \quad 0 < \zeta < 1. \tag{A.12}$$

By replacing (A.12) in (A.10)

$$x_{(n+1)} = x_{(n)} + T_0\left(u_{ez(n)}\cos(\psi_{ez(n)}) - \upsilon_{(n)}\sin(\psi_{(n)})\right) - T_0(e_{u(n)}\cos(\psi_{(n)}) - u_{ez(n)}e_{\psi(n)}\sin(\psi_{ez(n)} - \zeta e_{\psi(n)})). \tag{A.13}$$

By defining

$$f_{(n)} = -T_0(e_{u(n)}\cos(\psi_{(n)}) - u_{ez(n)}e_{\psi(n)}\sin(\psi_{ez(n)} - \zeta e_{\psi(n)})). \tag{A.14}$$

Then, considering (A.14) and $u_{ez(n)}$ from (20), and replacing in (A.13)

$$x_{(n+1)} = x_{(n)} + T_0\Bigg(\Bigg(\Bigg(\frac{y_{\text{ref}(n+1)} - k_y(y_{\text{ref}(n)} - y_{(n)}) - y_{(n)}}{T_0} - \upsilon_{(n)}\cos(\psi_{(n)})\Bigg)\sin(\psi_{ez(n)}) + \cdots + \Bigg(\frac{x_{\text{ref}(n+1)} - k_x(x_{\text{ref}(n)} - x_{(n)}) - x_{(n)}}{T_0} + \upsilon_{(n)}\sin(\psi_{(n)})\Bigg)\cos(\psi_{ez(n)})\Bigg) \times \cos(\psi_{ez(n)}) - \upsilon_{(n)}\sin(\psi_{(n)})\Bigg) + f_{(n)}. \tag{A.15}$$

From (18)

$$y_{\text{ref}(n+1)} - k_y(y_{\text{ref}(n)} - y_{(n)}) - y_{(n)} - \upsilon_{(n)}\cos(\psi_{(n)}) = \left(x_{\text{ref}(n+1)} - k_x(x_{\text{ref}(n)} - x_{(n)}) - x_{(n)} + \upsilon_{(n)}\sin(\psi_{(n)})\right) \times \frac{\sin(\psi_{ez(n)})}{\cos(\psi_{ez(n)})}. \tag{A.16}$$

Then, replacing (A.16) in (A.15)

$$x_{(n+1)} = x_{(n)} + T_0((x_{\text{ref}(n+1)} - k_x(x_{\text{ref}(n)} - x_{(n)}) - x_{(n)} + \upsilon_{(n)}\sin(\psi_{(n)})) \times \sin^2(\psi_{ez(n)}) + \cdots + (x_{\text{ref}(n+1)} - k_x(x_{\text{ref}(n)} - x_{(n)}) - x_{(n)} + \upsilon_{(n)}\sin(\psi_{(n)}))\cos^2(\psi_{ez(n)}) - \upsilon_{(n)}\sin(\psi_{(n)})) + f_{(n)}. \tag{A.17}$$

Then

$$x_{(n+1)} = x_{(n)} + T_0\left(x_{\text{ref(n+1)}} - k_x(x_{\text{ref}(n)} - x_{(n)}) - x_{(n)}\right) + f_{(n)}. \tag{A.18}$$

Operating

$$\underbrace{x_{\text{ref}(n+1)} - x_{(n+1)}}_{e_{x(n+1)}} = k_x(\underbrace{x_{\text{ref}(n)} - x_{(n)}}_{e_{x(n)}}) + f_{(n)}. \tag{A.19}$$

From (A.19)

$$e_{x(n+1)} - k_x e_{x(n)} + f_{(n)} = 0. \tag{A.20}$$

Finally, discuss e_y in the same way as the previous case. From the corresponding equation of (12)

$$y_{(n+1)} = y_{(n)} + T_0\left(u_{(n)}\sin(\psi_{(n)}) - \upsilon_{(n)}\cos(\psi_{(n)})\right). \tag{A.21}$$

Considering $e_{u(n)}$ from (A.1) and replacing in (A.21)

$$y_{(n+1)} = y_{(n)} + T_0\left(u_{ez(n)}\sin(\psi_{(n)}) + \upsilon_{(n)}\cos(\psi_{(n)})\right) - T_0 e_{u(n)}\sin(\psi_{(n)}). \tag{A.22}$$

The Taylor approximation of $\sin(\psi_{(n)})$ in the desired value $\psi_{ez(n)}$ is

$$\sin(\psi_{(n)}) = \sin(\psi_{ez(n)}) + \cos\left(\psi_{ez(n)} + \theta\left(\psi_{(n)} - \psi_{ez(n)}\right)\right) \times \left(\psi_{(n)} - \psi_{ez(n)}\right) \quad 0 < \theta < 1. \tag{A.23}$$

Considering $e_{\psi(n)}$

$$\sin(\psi_{(n)}) = \sin(\psi_{ez(n)}) + \cos\left(\psi_{ez(n)} + \theta e_{\psi(n)}\right) e_{\psi(n)} \quad 0 < \theta < 1. \tag{A.24}$$

By replacing (A.24) in (A.22)

$$y_{(n+1)} = y_{(n)} + T_0\left(u_{ez(n)}\sin(\psi_{ez(n)}) + \upsilon_{(n)}\cos(\psi_{(n)})\right) - T_0(e_{u(n)}\sin(\psi_{(n)}) - u_{ez(n)}e_{\psi(n)} \times \cos(\psi_{ez(n)} - \theta e_{\psi(n)})). \tag{A.25}$$

By defining

$$g_{(n)} = -T_0(e_{u(n)}\sin(\psi_{(n)}) - u_{ez(n)}e_{\psi(n)}\cos(\psi_{ez(n)} - \theta e_{\psi(n)})). \tag{A.26}$$

Then, considering (A.26) and $u_{ez(n)}$ from (20), and replacing in (A.25)

$$y_{(n+1)} = y_{(n)} + T_0\Bigg(\Bigg(\Bigg(\frac{y_{\text{ref}(n+1)} - k_y(y_{\text{ref}(n)} - y_{(n)}) - y_{(n)}}{T_0} - \upsilon_{(n)}\cos(\psi_{(n)})\Bigg)\sin(\psi_{ez(n)}) + \cdots + \Bigg(\frac{x_{\text{ref}(n+1)} - k_x(x_{\text{ref}(n)} - x_{(n)}) - x_{(n)}}{T_0} + \upsilon_{(n)}\sin(\psi_{(n)})\Bigg)\cos(\psi_{ez(n)})\Bigg)\sin(\psi_{ez(n)}) + \upsilon_{(n)}\sin(\psi_{(n)})\Bigg) + g_{(n)}. \tag{A.27}$$

Considering (18)

$$x_{\text{ref}(n+1)} - k_x(x_{\text{ref}(n)} - x_{(n)}) - x_{(n)} + \upsilon_{(n)}\sin(\psi_{(n)}) = \left(y_{\text{ref}(n+1)} - k_y(y_{\text{ref}(n)} - y_{(n)}) - y_{(n)} - \upsilon_{(n)}\cos(\psi_{(n)})\right) \times \frac{\cos(\psi_{ez(n)})}{\sin(\psi_{ez(n)})}. \tag{A.28}$$

Replace (A.28) in (A.27)

$$\begin{aligned} y_{(n+1)} = y_{(n)} + T_0((&y_{\text{ref}(n+1)} - k_y(y_{\text{ref}(n)} - y_{(n)}) - y_{(n)} \\ &- v_{(n)} \cos(\psi_{(n)})) \cos^2(\psi_{ez(n)}) + \cdots \\ &+ (y_{\text{ref}(n+1)} - k_y(y_{\text{ref}(n)} - y_{(n)}) - y_{(n)} \\ &- v_{(n)} \cos(\psi_{(n)})) \sin^2(\psi_{ez(n)}) \\ &+ v_{(n)} \sin(\psi_{(n)})) + g_{(n)}. \end{aligned} \tag{A.29}$$

Operating

$$y_{(n+1)} = y_{(n)} + T_0 \left(y_{\text{ref}(n+1)} - k_y(y_{\text{ref}(n)} - y_{(n)}) - y_{(n)}\right) + g_{(n)}. \tag{A.30}$$

From (A.30)

$$\underbrace{y_{\text{ref}(n+1)} - y_{(n+1)}}_{e_{y(n+1)}} = k_y(\underbrace{y_{\text{ref}(n)} - y_{(n)}}_{e_{y(n)}}) + g_{(n)}. \tag{A.31}$$

Finally, we get

$$e_{y(n+1)} - k_y e_{y(n)} + g_{(n)} = 0. \tag{A.32}$$

Considering (A.14), (A.20), (A.26), and (A.32), we get

$$\begin{aligned} \begin{bmatrix} e_{x(n+1)} \\ e_{y(n+1)} \end{bmatrix} &= \underbrace{\begin{bmatrix} k_x & 0 \\ 0 & k_y \end{bmatrix} \begin{bmatrix} e_{x(n)} \\ e_{y(n)} \end{bmatrix}}_{\text{Linear System}} \\ &+ T_0 \underbrace{\begin{bmatrix} -u_{ez(n)} \sin\left(\psi_{ez(n)} - \zeta e_{\psi(n)}\right) & \cos(\psi_{(n)}) \\ -u_{ez(n)} \cos\left(\psi_{ez(n)} - \theta e_{\psi(n)}\right) & \sin\left(\psi_{(n)}\right) \end{bmatrix} \begin{bmatrix} e_{\psi(n)} \\ e_{u(n)} \end{bmatrix}}_{\text{Nonlinearity}}. \end{aligned} \tag{A.33}$$

Equation (A.33) represents a linear system and a nonlinearity, if $0 < k_x, k_y < 1$, then (A.33) tends to zero because $e_{\psi(n)}$ and $e_{u(n)} \to 0$ when $n \to 0$. Finally, because $e_{\psi(n)}$ and $e_{u(n)} \to 0$ when $n \to 0$ is demonstrated that $e_{x(n)}$ and $e_{y(n)} \to 0$ when $n \to 0$, and the tracking error tends to 0.

References

[1] S. Oh and J. Sun, “Path following of underactuated marine surface vessels using line-of-sight based model predictive control,” *Ocean Eng.*, vol. 37, nos. 2–3, pp. 289–295, Feb. 2010.

[2] J. Ghommam, F. Mnif, and N. Derbel, “Global stabilisation and tracking control of underactuated surface vessels,” *IET Control Theory Appl.*, vol. 4, no. 1, pp. 71–88, Jan. 2010.

[3] K. D. Do, Z. P. Jiang, and J. Pan, “Universal controllers for stabilization and tracking of underactuated ships,” *Syst. Control Lett.*, vol. 47, no. 4, pp. 299–317, Nov. 2002.

[4] M. Wondergem, E. Lefeber, K. Y. Pettersen, and H. Nijmeijer, “Output feedback tracking of ships,” *IEEE Trans. Control Syst. Technol.*, vol. 19, no. 2, pp. 442–448, Mar. 2011.

[5] Z. P. Jiang, “Global tracking control of underactuated ships by Lyapunov’s direct method,” *Automatica*, vol. 38, no. 2, pp. 301–309, Feb. 2002.

[6] K. D. Do, Z. P. Jiang, and J. Pan, “Robust global stabilization of underactuated ships on a linear course: State and output feedback,” in *Proc. Process. Amer. Control Conf.*, 2002, pp. 1687–1692.

[7] J. Ghommam, F. Mnif, A. Benali, and N. Derbel, “Asymptotic backstepping stabilization of an underactuated surface vessel,” *IEEE Trans. Control Syst. Technol.*, vol. 14, no. 6, pp. 1150–1157, Nov. 2006.

[8] M. Bao-Li, “Global *k*-exponential asymptotic stabilization of underactuated surface vessels,” *Syst. Control Lett.*, vol. 58, no. 3, pp. 194–201, Mar. 2009.

[9] K. P. Tee and S. S. Ge, “Control of fully actuated ocean surface vessels using a class of feedforward approximators control of fully actuated ocean surface vessels using a class of feedforward approximators,” *IEEE Trans. Control Syst. Technol.*, vol. 14, no. 4, pp. 750–756, Jul. 2006.

[10] L. Yu-Lei, W. Lei, and Z. Jia-Yuan, “Backstepping dynamical sliding mode control method for the path following of the underactuated surface vessel,” *Procedia Eng.*, vol. 15, pp. 256–263 , Dec. 2011.

[11] L. Lapierre and B. Jouvencel, “Robust nonlinear path-following control of an AUV,” *IEEE J. Ocean. Eng.*, vol. 33, no. 2, pp. 89–102, Apr. 2008.

[12] G. Scaglia, L. Quintero, V. Mut, and F. di Sciascio, “Numerical methods based controller design for mobile robots,” in *Proc. 17th World Congr. IFAC*, Jul. 2008, pp. 4820–4827.

[13] G. Scaglia, L. Quintero, V. Mut, and F. di Sciascio, “Numerical methods based controller design for mobile robots,” *Robotica*, vol. 27, no. 02, pp. 269–279, Mar. 2009.

[14] A. Rosales, G. Scaglia, V. Mut, and F. di Sciascio, “Formation control and trajectory tracking of mobile robotic systems—A linear algebra approach,” *Robotica*, vol. 29, no. 3, pp. 335–349, May 2011.

[15] E. Børhaug, A. Pavlov, E. Panteley, and K. Y. Pettersen, “Straight line path following for formations of underactuated marine surface vessels,” *IEEE Trans. Control Syst. Technol.*, vol. 19, no. 3, pp. 493–506, May 2011.

[16] T. I. Fossen, *Marine Control Systems*. Trondheim, Norway: Marine Cybernetics, 2002.

[17] G. Strang, *Linear Algebra and Its Applications*. San Francisco, CA, USA: Academic, 1980.

[18] Y. Zheng and W. Jun, “Model predictive control for tracking of underactuated vessels based on recurrent neural networks,” *IEEE J. Ocean. Eng.*, vol. 37, no. 4, pp. 717–726, Oct. 2012.